


Berry Phase of Phonons and Thermal Hall Effect in Nonmagnetic Insulators

Takuma Saito,¹ Kou Misaki,¹ Hiroaki Ishizuka,¹ and Naoto Nagaosa^{1,2}

¹*Department of Applied Physics, The University of Tokyo, Bunkyo-ku, Tokyo, 113-8656, Japan*

²*RIKEN Center for Emergent Matter Science (CEMS), Wako, Saitama, 351-0198, Japan*

 (Received 25 January 2019; published 18 December 2019)

A mechanism for the phonon Hall effect (PHE) in nonmagnetic insulators under an external magnetic field is theoretically studied. PHE is known in (para)magnetic compounds, where the magnetic moments and spin-orbit interaction play an essential role. In sharp contrast, we here discuss that the PHE also occurs in nonmagnetic band insulators subject to the magnetic field. We find that a correction to the Born-Oppenheimer approximation gives rise to a Raman-type interaction between the magnetic field and the phonons; this interaction gives rise to the Berry curvature of a phonon band. This Berry curvature results in the finite thermal Hall conductivity κ_H in nonmagnetic band insulators. The value of κ_H is calculated for square and honeycomb lattices. The order of the magnitude estimation for κ_H is given for Si at room temperature.

DOI: 10.1103/PhysRevLett.123.255901

Introduction.—Hall effects are one of the most important subjects in condensed matter physics. They provide the information on the sign and density of the carriers in semiconductors, and the shape of the Fermi surface in metals. Since the discovery of the quantum Hall effect [1], the close connection of Hall effects to the topological nature of electronic states in solids has become a keen issue. In addition to the quantum Hall effect, the anomalous Hall effect in metallic magnets [2], and spin Hall effect in semiconductors [3] are interpreted as the consequence of the geometric phase of Bloch wave functions, i.e., the Berry phase in solids [4]. The Berry phase can be nonzero even for neutral particles such as photons [5] and magnons [6–9], and the Hall effects of these particles are observed experimentally in Refs. [10,11], respectively.

Phonon is another neutral particle in solids, and the thermal Hall effect of phonons, phonon Hall effect, has been studied experimentally [12,13] and theoretically [14–22]. In most of the theoretical works the intrinsic Hall effect is studied. Particularly, the Raman-type interaction is often assumed whose Hamiltonian reads

$$H_{\text{Raman}} = \lambda \mathbf{M} \cdot (\mathbf{u} \times \mathbf{P}), \quad (1)$$

where \mathbf{M} is the electronic magnetization, \mathbf{u} the displacement of the nucleus, and \mathbf{P} the momentum of the nucleus. This coupling λ is supposed to originate from the spin-lattice interaction, but the microscopic theory for λ is missing in most of the cases.

The charge of the phonon, however, is a subtle issue because the atomic nuclei are positively charged, which is compensated by the electrons. Then the screening effect of electrons should be treated properly to ensure the neutral nature of phonons. The conventional formalism to study the electron-phonon coupled system is the Born-Oppenheimer (BO) approximation [23], which uses the fact that the

electron mass m is much lighter than that of atoms M . Writing the wave function as the product of the electronic and nuclear part, i.e., $\Psi(r, R) = \psi_{\text{el}}(r, R)\phi_{\text{nucl}}(R)$ with r and R being the position of electrons and nuclei, respectively, the ratio of the length scales ℓ_{el} and ℓ_{nucl} for $\psi_{\text{el}}(r, R)$ and $\phi_{\text{nucl}}(R)$ is estimated as

$$\ell_{\text{el}}/\ell_{\text{nucl}} \sim (m_{\text{nucl}}/m_{\text{el}})^{1/4}. \quad (2)$$

Therefore, the derivative ∇_R on $\psi_{\text{el}}(r, R)$ can seemingly be neglected and the Schrödinger equation for $\phi_{\text{nucl}}(R)$ contains the information of electrons only through the ground state energy $E(R)$ of electrons which depends on the nuclear position R regarded as the static parameter. In this approximation, however, the nucleus feels the external electromagnetic field as the particle with positive charge Ze . This drawback can be remedied by introducing the Berry phase into the Hamiltonian of the nucleus [23].

$$H_{\text{nucl}} = \sum_n \frac{[\mathbf{P}_n - Ze\mathbf{A}_n - \mathbf{a}_n(R)]^2}{2m_{\text{nucl}}} + U(R), \quad (3)$$

where n specifies the atom and $R = (\mathbf{R}_1, \dots, \mathbf{R}_N)$ represents the coordinates of all the N atoms. Here, $\mathbf{a}_n(R)$ is the Berry connection given by

$$\mathbf{a}_n^\alpha(R) = i\hbar \left\langle \psi_{\text{el}}(r, R) \left| \frac{\partial}{\partial R_n^\alpha} \psi_{\text{el}}(r, R) \right. \right\rangle, \quad (4)$$

where $|\psi_{\text{el}}(R)\rangle$ is the state of electrons with a dependence on nuclear coordinates. $U(R)$ is the sum of the electronic ground state energy and the interaction between nuclei.

This $\mathbf{a}_n(R)$ cancels the vector potential \mathbf{A}_n for the external electromagnetic field in the case of a single atom; i.e., the screening of the positive charge of the nucleus by

electrons is recovered [23]. For the hydrogen molecule, it has been discussed that this screening is perfect for the center-of-mass motion while the magnetic field effect survives for the relative motion of the two atoms [24]. Therefore, the effect of the magnetic field on the phonons in crystal remains an important issue to be studied.

In the present Letter, we study theoretically the Berry phase appearing in the phonon Hamiltonian and the consequent thermal Hall effect in a trivial band insulator. Our model is the spinless fermion model with an s orbital at each site, and there are no magnetic moments or spin-orbit interactions. Therefore, the effect of the magnetic field is only through the orbital motion of electrons and nuclei. As for the electrons, the Lorentz force is acting to produce the weak orbital diamagnetism but there is no thermal Hall effect because of the energy gap in the low temperature limit. As for the phonons, on the other hand, the acoustic phonons have gapless dispersions, and hence can be excited thermally even at a low temperature.

Berry curvature and screening.—From the Berry connection given in Eq. (4), we obtain the Berry curvature $F_{\mu\nu}$ as

$$\begin{aligned} F_{\mu\nu} &= \partial_\mu a_\nu - \partial_\nu a_\mu \\ &= -2\hbar \text{Im} \langle \partial_\mu \psi_{\text{el}}(r, R) | \partial_\nu \psi_{\text{el}}(r, R) \rangle. \end{aligned} \quad (5)$$

Here, we introduced the symbol $\mu = (n, \alpha)$ for the α component of the n th nucleus. Therefore, $F_{\mu\nu}$ is the tensor with $3N \times 3N$ components. We also denote it by $F_{nm}^{\alpha\beta}$ in order to emphasize the nuclear and spacial indices. We note that, as mentioned by Resta [25], $F_{\mu\nu}$ is antisymmetric for the exchange of μ and ν , but not for α and β , i.e., the condition

$$F_{nm}^{\alpha\beta} = -F_{nm}^{\beta\alpha} = F_{mn}^{\alpha\beta} \quad (6)$$

is not always true.

From Eq. (3), we obtain the equation of motion of nuclei:

$$M\ddot{R}_n^\alpha = -\partial_{n\alpha} U + \epsilon^{\alpha\beta\gamma} V_n^\beta Z e B^\gamma - \sum_m V_m^\beta F_{nm}^{\alpha\beta},$$

where V_n indicates the velocity of nuclei n . When Eq. (6) holds, one can define a vector $b_{nm}^\alpha := \frac{1}{2} \epsilon^{\alpha\beta\gamma} F_{nm}^{\beta\gamma} = \frac{1}{2} \epsilon^{\alpha\beta\gamma} F_{mn}^{\beta\gamma}$, by which the last term turns into $\sum_m \epsilon^{\alpha\beta\gamma} V_m^\beta b_{nm}^\gamma$. This means that b_{nm} works as an effective magnetic field in the system and induces effective Lorentz force.

In a hydrogenlike atom under a magnetic field, the Berry curvature contribution cancels the external magnetic field [23]. The key point is the $U(1)$ phase attached to the wave function due to the magnetic field. The atomic orbital $\varphi(\mathbf{r} - \mathbf{R})$ acquires an extra phase under the magnetic field:

$$\varphi(\mathbf{r} - \mathbf{R}) \rightarrow \varphi'(\mathbf{r}, \mathbf{R}) = \varphi(\mathbf{r} - \mathbf{R}) e^{(ie/\hbar)\mathbf{A}(\mathbf{R})\cdot\mathbf{r}}. \quad (7)$$

Here, we have fixed the gauge and used the symmetric gauge. Although the manner of attaching the phase is a subtle problem, it is known that, as for the symmetric gauge, Eq. (7) yields physically correct results up to the B -linear order. In calculating the curvature, the derivative with respect to the nuclear coordinates is modified by this additional phase, which extracts the effect from the magnetic field.

On the other hand, the situation is quite different if the system contains two or more nuclei. In the hydrogen molecule, for instance, cancellation of the external magnetic field and the Berry curvature is perfect for the translational motion, but not for the relative motion of the two nuclei [24]. In general cases, the screening of the magnetic field is guaranteed only for the translational motion, described by

$$\sum_{nm} F_{nm}^{\alpha\beta} = -N \epsilon^{\alpha\beta\gamma} Z e B^\gamma. \quad (8)$$

Estimation of the Berry curvature.—As a simple estimation of the Berry curvature $F_{\mu\nu}$, we here study the Berry curvature of phonons in a two-dimensional square and honeycomb lattice with N nuclei and the same number of spinless electrons. (The discussion below can be similarly applied to other lattice structures.) Each electron is tightly bound to each atom, and then the wave function for the noninteracting electrons is given by the Slater determinant of the wave functions of all the N atoms. We denote the single-particle state of the i th electron at the n th nucleus by $\phi_{in} = \varphi'(r_i, R_n)$, given in Eq. (7). The many-body wave function is proportional to the determinant of $\Phi(r, R)$, an $N \times N$ matrix whose (i, n) component is given by ϕ_{in} . Although this model is very simple, the microscopic mechanism discussed here is ubiquitous and applicable to any materials.

The key factor which characterizes the Berry curvature of electron-phonon coupled systems is the overlap integral between the orbitals of the n th and m th atoms, which we denote by S_{nm} . The overlap integral is affected by the additional phase factor of the atomic orbital under the magnetic field. The modified overlap integral $S'_{nm} := \int d^3r_i \phi_{in}^* \phi_{im}$ is given by $S_{nm}' = S_{nm} e^{i\theta_{nm}} + \mathcal{O}(B^2)$, where $\theta_{nm} := (e/\hbar)\mathbf{A}(\mathbf{R}_n) \cdot \mathbf{R}_m$. For brevity, we here define two matrices, S and S' , whose (n, m) components are S_{nm} and S'_{nm} , respectively.

The normalized wave function of this system is given by $\psi_{\text{el}}(r, R) = (N! \det S')^{-1/2} \det \Phi(r, R)$. The general formula of $F_{\mu\nu}$ of lattice systems is obtained by substituting $\psi_{\text{el}}(r, R)$ into Eq. (5), which is reduced to simpler formulas in concrete models, the details of which are given in the Supplemental Material [26]. Here, we assume that the overlap integral between the nearest-neighbor nuclei is dominant. Furthermore, we consider s orbitals, which are isotropic and real valued. Under this assumption, $F_{\mu\nu}$ for the square lattice is obtained up to the linear order in B [26]:

$$a_n^\alpha = -e \left(A_n^\alpha (S^{-1})_{nn} + \sum_{l \neq n} A_l^\alpha (S^{-1})_{nl} S_{nl} \right), \quad (9a)$$

$$F_{nm}^{\alpha\beta} = -(S^{-1})_{nn} \epsilon^{\alpha\beta\gamma} e B^\gamma - \sum_l (S^{-1})_{nl} [-e(A_n^\beta - A_l^\beta) \partial_{n\alpha} S_{nl} + e(A_n^\alpha - A_l^\alpha) \partial_{n\beta} S_{nl}], \quad (9b)$$

$$F_{nm}^{\alpha\beta} = -(S^{-1})_{nm} [\epsilon^{\alpha\beta\gamma} e B^\gamma S_{nm} + e(A_n^\beta - A_m^\beta) \partial_{n\alpha} S_{nm} - e(A_n^\alpha - A_m^\alpha) \partial_{m\beta} S_{nm}]. \quad (9c)$$

Here, we abbreviated $A^\alpha(\mathbf{R}_n)$ to A_n^α . Equations (9b) and (9c) imply that the curvature is mainly dependent on the overlap integral and its derivative. The obtained expression of $F_{nm}^{\alpha\beta}$ is antisymmetric for the exchange of α and β , and hence we can define a vector $b_{nm}^\alpha := \frac{1}{2} \epsilon^{\alpha\beta\gamma} F_{nm}^{\beta\gamma}$, the curvature felt by nucleus n and caused by nucleus m . \mathbf{b}_{nm} is parallel to \mathbf{B} , and the magnetic screening effect,

$$\sum_m \mathbf{b}_{nm} = -e\mathbf{B}, \quad (10)$$

is guaranteed, as in Eq. (8) ($Z = 1$ in this model).

Effective Hamiltonian for the band insulator.—The effective Hamiltonian for the phonons is obtained by considering a small deviation \mathbf{u}_n of the nuclei from its ground state position \mathbf{R}_n^0 ; $\mathbf{R}_n = \mathbf{u}_n + \mathbf{R}_n^0$. As for the interaction among nuclei, only quadratic terms of u_n^α 's are taken into account. The Berry curvature at the equilibrium atomic positions,

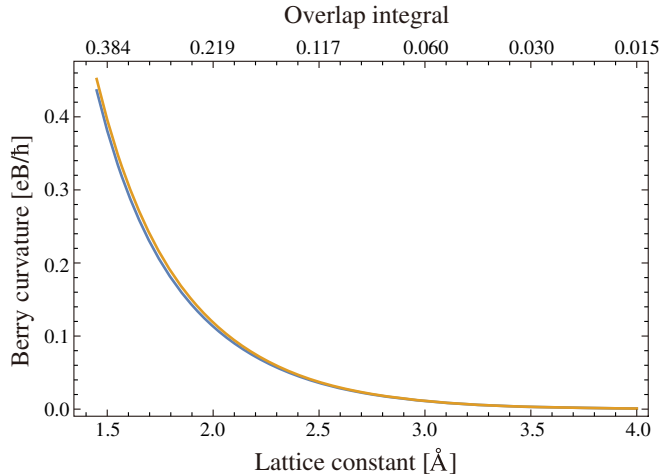


FIG. 1. The Berry curvature of the nearest-neighbor 1s orbitals, $F_{nm}^{\alpha\beta}$ (or, equivalently, b_{nm}^α), is plotted with respect to the lattice constant. The blue line corresponds to the square lattice, and the orange one to the honeycomb lattice, where there is little difference. The unit of the vertical axis is eB/\hbar . For the horizontal axis, the lower and upper axes show the lattice constants and the corresponding values of the overlap integral.

i.e., $F_{nm}^{\alpha\beta}|_{R=R^0}$, is included in the Hamiltonian by the minimal coupling, as in Eq. (3). Hereafter, we omit “ $R = R^0$ ” and always take this substitution without notice. Figure 1 shows the numerical evaluation of $F_{nm}^{\alpha\beta}$ for the nearest-neighbor pair (n, m) . The Berry connection can be expressed by using \mathbf{b}_{nm} up to the linear order of u_n^α :

$$\mathbf{a}_n = \sum_m \frac{1}{2} \mathbf{b}_{nm} \times \mathbf{R}_m = \sum_m \frac{1}{2} \mathbf{b}_{nm} \times \mathbf{u}_m + (\text{const}), \quad (11)$$

where the constant term can be removed by gauge transformation. Combining the contributions from the external magnetic field and the Berry curvature, the effective vector potential becomes

$$\mathbf{a}'_n := e\mathbf{A}(\mathbf{R}_n) + \mathbf{a}_n = \frac{1}{2} \sum_m \mathbf{b}_{nm} \times (\mathbf{u}_m - \mathbf{u}_n). \quad (12)$$

In the second line, we used the identity equation (10).

The Hamiltonian of the lattice vibration is modified in the existence of \mathbf{a}'_n : the resultant Hamiltonian for our model is given by

$$H_{\text{nucl}} = \sum_n \left(\frac{(\mathbf{P}_n - \mathbf{a}'_n)^2}{2m_{\text{nucl}}} + \frac{1}{2} \sum_m \mathbf{u}_n^T D_{nm} \mathbf{u}_m \right) \quad (13a)$$

$$= \sum_k \left(\frac{1}{2m_{\text{nucl}}} \Pi_k^{\alpha\dagger} \Pi_k^\alpha + \frac{1}{2} D_k^{\alpha\beta} u_k^{\alpha\dagger} u_k^\beta \right), \quad (13b)$$

where $\Pi_k := P_k - a'_k$ is the momentum under a magnetic field. It is noted that the commutation relationship of u_k and Π_k is different from that of usual canonical operators: $[u_k^\alpha, u_q^\beta] = 0$, $[u_k^\alpha, \Pi_q^\beta] = i\hbar$, and $[\Pi_k^\alpha, \Pi_q^\beta] = i\hbar G_k^{\alpha\beta}$, where $G_k^{\alpha\beta} := \partial_{k\alpha} a'_k{}^\beta - \partial_{k\beta} a'_k{}^\alpha$. We can see that the effective vector potential plays a role of the Raman interaction. Compared with the original Raman interaction, \mathbf{a}'_n does not include k -independent constant terms but a second-order derivative, so that it vanishes in the $k \rightarrow 0$ limit. This is consistent with Eq. (45) of Ref. [20].

Thermal Hall effect.—The effective vector potential \mathbf{a}'_n induces the thermal Hall effect of phonons. In this section, we derive the analytic expression for the thermal Hall conductance κ_H and numerically estimate it.

The definition of energy current in lattice systems, which we denote \mathbf{J}_E , was given by Hardy [31] as an operator satisfying the local energy conservation law. In addition to the usual Kubo formula, we have to take into account the contribution from the energy magnetization \mathbf{M}_E , defined by $\mathbf{J}_E = \nabla \times \mathbf{M}_E$ [32]. The complete formula for the thermal Hall conductance is given by

$$\kappa_H^{\text{tr}} = \kappa_H^{\text{Kubo}} + \frac{2M_E^z}{TV}.$$

The detailed calculation was given by Qin *et al.* [20]. The general formula for the thermal Hall conductance of bosonic particles is

$$\kappa_H^{\text{tr}} = -\frac{(\pi k_B)^2 T}{3\hbar} Z_{\text{ph}} - \frac{1}{T} \int_0^\infty d\epsilon \epsilon^2 \sigma_{xy}(\epsilon) \frac{dn_B(\epsilon)}{d\epsilon}, \quad (14)$$

where $Z_{\text{ph}} := \sum_{i \in \text{particle bands}} (1/V) \sum_{\mathbf{k} \in \text{BZ}} \Omega_{\mathbf{k}i}^z$ and $\sigma_{xy}(\epsilon) := (-1/V\hbar) \sum_{\hbar\omega_{ki} \leq \epsilon} \Omega_{\mathbf{k}i}^z$. Here, ω_{ki} is the frequency of the phonon of the i th mode and $n_B(\epsilon) = 1/(e^{\beta\epsilon} - 1)$ is the Bose distribution. The Berry curvature of phonons is defined as follows [17,20]: we define two matrices $\mathcal{A}_{\mathbf{k}}$ and $\mathcal{B}_{\mathbf{k}}$ by $\mathcal{A}_{\mathbf{k}} = i\hbar \begin{bmatrix} O & I_2 \\ -I_2 & G_{\mathbf{k}} \end{bmatrix}$ and $\mathcal{B}_{\mathbf{k}} = \begin{bmatrix} D_{\mathbf{k}} & O \\ O & m_{\text{nuc}i}^{-1} I_2 \end{bmatrix}$, where I_2 is the 2×2 identity matrix. From the equation of motion, the eigenenergy is obtained by diagonalizing $\tilde{H}_{\mathbf{k}} := \mathcal{A}_{\mathbf{k}} \mathcal{B}_{\mathbf{k}}$. We denote the eigenvectors of $\tilde{H}_{\mathbf{k}}$ by $|v_i\rangle$. Then the Berry connection and curvature are defined by

$$a_{ki}^\alpha := -\text{Im}\langle v_i | \mathcal{B}_{\mathbf{k}} \partial_{k\alpha} | v_i \rangle, \quad (15a)$$

$$\Omega_{\mathbf{k},i}^z := \partial_{k_x} a_{ki}^y - \partial_{k_y} a_{ki}^x. \quad (15b)$$

The first term in Eq. (14) consists of a summation of Berry curvature over the Brillouin zone and over all the particle bands, Z_{ph} . In the previous study, Z_{ph} is supposed to vanish in most cases [20]. For the case of magnonic systems, the summation of the Chern number over particle bands is exactly zero [33]. This can be explained by the fact that the Bogoliubov–de Gennes Hamiltonian of the system is adiabatically connected to a trivial matrix, whose Berry curvature is zero. A parallel discussion leads to the conclusion that $Z_{\text{ph}} = 0$ holds exactly in our model [26], if we perturb the system to introduce the gap at $\mathbf{k} = 0$ so that the Chern number is well defined.

We here apply the continuum approximation in order to see the behavior of κ_H at low temperature and identify on which factors κ_H is dependent. The dynamical matrix and the vector potential of the general Hamiltonian of phonons with Raman-type interaction are given by $D_{\mathbf{k}}^{\alpha\beta} = \mu_1 k^2 \delta^{\alpha\beta} + \mu_2 k^\alpha k^\beta$ and $a_{\mathbf{k}}^\alpha = \gamma_1 \partial_\alpha \partial_\beta \epsilon^{\beta\rho\sigma} M^\rho u^\sigma + \gamma_2 \nabla^2 \epsilon^{\alpha\beta\gamma} M^\beta u^\gamma$ in Eq. (13b), where γ_1 and γ_2 are coupling constants [20]. The corresponding geometric curvature is $G_{\mathbf{k}}^{\alpha\beta} = (1/m_{\text{nuc}i}) \epsilon^{\alpha\beta\gamma} [-\gamma_1 k^\gamma \mathbf{k} \cdot \mathbf{M} + (\gamma_1 + 2\gamma_2) k^2 M^\gamma]$. The continuum approximation is valid when the temperature is sufficiently low, i.e., $\Theta_D \gg T$ ($\Theta_D := \hbar c_T \pi / a k_B$ is the Debye temperature, where c_T is the sound velocity of the transverse acoustic mode). Under these conditions, the thermal Hall conductance in two dimensions reads

$$\kappa_H^{2D} = \frac{\pi^2 k_B}{m_{\text{nuc}i} \Theta_D^2} \Gamma^{2D} T^2 \int_0^\infty dx \frac{x^3 e^x}{(e^x - 1)^2}. \quad (16)$$

Γ^{2D} is a constant dependent on the ratio of sound speed of the longitudinal and transverse modes, $\delta := c_L/c_T$, which is given by

$$\Gamma^{2D} = 2\pi(2\gamma_2 - \gamma_1) M^z \frac{(\delta - 1)^2}{\delta(\delta + 1)}. \quad (17)$$

Now, we apply the discussion above to our model. In nonmagnetic insulators, the geometric curvature \mathbf{b}_{nm} plays the role of the magnetization \mathbf{M} , and it takes finite value only for the nearest-neighbor nuclei. We here denote \mathbf{b}_{nm} of the nearest-neighbor nuclei by \mathbf{b} . The sum over m in Eq. (12) is reduced to the sum over the nearest-neighbor nuclei; i.e., m is an integer which satisfies $\mathbf{R}_m^0 = \mathbf{R}_n^0 \pm \mathbf{e}_x, \mathbf{R}_m^0 \pm \mathbf{e}_y$, where \mathbf{e}_x (\mathbf{e}_y) is the lattice vector for the x (y) direction. Assuming \mathbf{u}_n is a slowly varying parameter of \mathbf{R}_n , we expand it by the gradient as $u_{n\pm x(y)}^\alpha \simeq u_n^\alpha \pm a \partial_{x(y)} u_n^\alpha + (a^2/2) \partial_{x(y)}^2 u_n^\alpha$. Then the vector potential (12) becomes

$$\mathbf{a}'(\mathbf{R}) = a^2 \mathbf{b} \times \nabla^2 \mathbf{u}(\mathbf{R}). \quad (18)$$

Therefore, the coupling constants are replaced as $\gamma_1 \rightarrow 0$ and $\gamma_2 M^z \rightarrow a^2 b^z$ (in the honeycomb lattice, a prefactor $2/3$ is attached to γ_2). Equation (16) implies that the factors which dominate the value of κ_H are (i) the sound velocity of phonons and the ratio of that of longitudinal and transverse modes, (ii) the mass of nuclei, and (iii) the screening of the magnetic field, which is determined by the overlap integral of atomic orbitals between neighboring sites.

Figure 2 shows our calculation of the thermal Hall conductivity in the lattice models. Here, the thermal Hall conductivity in two dimensions κ_H^{2D} is translated into the thermal Hall conductivity in three dimensions κ_H by assuming that the thickness of the layer is almost the same

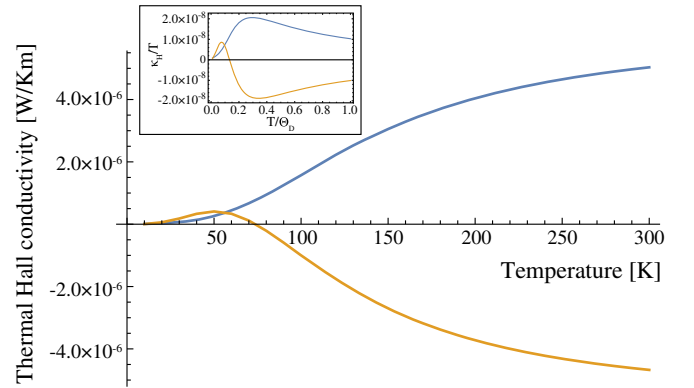


FIG. 2. The thermal Hall conductance of the lattice models under $B = 10$ (T) is plotted with respect to temperature. The blue and orange lines correspond to square and honeycomb lattices, respectively. The inset shows the plot of κ_H/T with respect to dimensionless temperature T/Θ_D . It can be seen to what temperature the T^2 law $\kappa_H \propto T^2$, i.e., the continuum approximation equation (16) holds. With our choice of the parameters [see the main text], $\Theta_D = 216$ K.

as the lattice constant, i.e., $\kappa_H := \kappa_H^{2D}/a$. One can see different behaviors of κ_H in the square and honeycomb lattices. This is due to the two kinds of the divergence in $\Omega_{k,i}^z$: one comes from the Γ point, which exists in any lattice structure, while the other comes from the anticrossing point of two bands along the high symmetry line [26]. The Berry curvature of the optical bands is much larger than that of the acoustic bands, which is similar to the angular momentum of the phonon [34]. Thus, the contribution from the anticrossing point becomes dominant at higher temperatures. Moreover, it has a negative sign, as can be seen in the magnon Hall effect in a Kagome magnet [35].

Let us explain how we determine the parameters used to obtain the results in Fig. 2. Materials well described by our model are monatomic, nonmagnetic band insulators, and one candidate material is Si crystal: although the lattice structure is different from square or honeycomb lattices, we believe the order of the magnitude estimation of κ_H is approximately estimated by our model. Thus, the parameters used in the calculation are $a = 2.31 \text{ \AA}$, m_{nuc} equals 28 times proton mass, and the spring constants between nearest neighbor and next-nearest neighbor are chosen so that the sound velocities satisfy $c_T \sim 5 \times 10^3 \text{ m/s}$ and $c_L \sim 9 \times 10^3 \text{ m/s}$. The outermost electrons in Si crystal form the hybridization of $3s$ and $3p$ orbitals, i.e., so-called sp_3 orbitals. For simplicity, we here estimate the overlap using the $3s$ orbital with an effective charge $Z = 4.15$, which results from the Slater rule, and obtain $S = 0.35$. Using this, the Berry curvature is estimated to be $b^z \sim 0.3eB/\hbar$. The resultant thermal Hall conductance is $\kappa_H \sim 10^{-6} \text{ W/Km}$ at $T = 300 \text{ K}$. This can be distinguished from the contribution from thermally excited electrons and holes $\kappa_H^{\text{el,h}}$, which is estimated to be much smaller. In Si, for example, the intrinsic carrier concentration is $n_i = 10^{10} \text{ cm}^{-3}$ at $T = 300 \text{ K}$ [36], and $\kappa_H^{\text{el,h}} \sim 10^{-9} \text{ W/Km}$ at $B = 10 \text{ T}$ [26]. Thus, we believe the phonon Hall effect is detectable at higher temperatures and with a larger temperature gradient.

This work was supported by JSPS KAKENHI Grants No. JP18H03676, No. JP18H04222, No. JP24224009, and No. JP26103006, ImPACT Program of Council for Science, Technology and Innovation (Cabinet office, Government of Japan), and CREST, JST (Grant No. JPMJCR1874). T.S. was supported by Japan Society for the Promotion of Science through Program for Leading Graduate Schools (MERIT).

[1] For a recent review, see *Quantum Hall Effect*, edited by R. E. Prange and S. M. Girvin (Springer-Verlag, New York, 1990).

[2] N. Nagaosa, J. Sinova, S. Onoda, A. H. MacDonald, and N. P. Ong, *Rev. Mod. Phys.* **82**, 1539 (2010).

- [3] S. Murakami and N. Nagaosa, in *Comprehensive Semiconductor Science and Technology*, edited by R. Fornari and H. Kamimura (Elsevier, Amsterdam, 2011), p. 222.
- [4] D. Xiao, M.-C. Chang, and Q. Niu, *Rev. Mod. Phys.* **82**, 1959 (2010).
- [5] M. Onoda, S. Murakami, and N. Nagaosa, *Phys. Rev. Lett.* **93**, 083901 (2004).
- [6] H. Katsura, N. Nagaosa, and P. A. Lee, *Phys. Rev. Lett.* **104**, 066403 (2010).
- [7] R. Matsumoto and S. Murakami, *Phys. Rev. Lett.* **106**, 197202 (2011).
- [8] R. Matsumoto and S. Murakami, *Phys. Rev. B* **84**, 184406 (2011).
- [9] R. Matsumoto, R. Shindou, and S. Murakami, *Phys. Rev. B* **89**, 054420 (2014).
- [10] O. Hosten and P. Kwiat, *Science* **319**, 787 (2008).
- [11] Y. Onose, T. Ideue, H. Katsura, Y. Shiomi, N. Nagaosa, and Y. Tokura, *Science* **329**, 297 (2010).
- [12] C. Strohm, G. L. J. A. Rikken, and P. Wyder, *Phys. Rev. Lett.* **95**, 155901 (2005).
- [13] A. V. Inyushkin and A. Taldenkov, *JETP Lett.* **86**, 379 (2007).
- [14] L. Sheng, D. N. Sheng, and C. S. Ting, *Phys. Rev. Lett.* **96**, 155901 (2006).
- [15] Y. Kagan and L. A. Maksimov, *Phys. Rev. Lett.* **100**, 145902 (2008).
- [16] J.-S. Wang and L. Zhang, *Phys. Rev. B* **80**, 012301 (2009).
- [17] L. Zhang, J. Ren, J.-S. Wang, and B. Li, *Phys. Rev. Lett.* **105**, 225901 (2010).
- [18] B. K. Agarwalla, L. Zhang, J.-S. Wang, and B. Li, *Eur. Phys. J. B* **81**, 197 (2011).
- [19] R. d. L. Kronig, *Physica (Utrecht)* **6**, 33 (1939).
- [20] T. Qin, J. Zhou, and J. Shi, *Phys. Rev. B* **86**, 104305 (2012).
- [21] M. Mori, A. Spencer-Smith, O. P. Sushkov, and S. Maekawa, *Phys. Rev. Lett.* **113**, 265901 (2014).
- [22] X. Zhang, Y. Zhang, S. Okamoto, and D. Xiao, *Phys. Rev. Lett.* **123**, 167202 (2019).
- [23] C. A. Mead, *Rev. Mod. Phys.* **64**, 51 (1992).
- [24] D. Ceresoli, R. Marchetti, and E. Tosatti, *Phys. Rev. B* **75**, 161101(R) (2007).
- [25] R. Resta, *J. Phys. Condens. Matter* **12**, R107 (2000).
- [26] See Supplemental Material at <http://link.aps.org/supplemental/10.1103/PhysRevLett.123.255901> for the derivation of the Berry curvature for general lattice systems (Sec. I), an argument for $Z_{\text{ph}} = 0$ (Sec. II), phonon band structure of our honeycomb lattice (Sec. III), and estimate of $\kappa_H^{\text{el,h}}$ (Sec. IV), which includes Refs. [27–30].
- [27] L. Faddeev and R. Jackiw, *Phys. Rev. Lett.* **60**, 1692 (1988).
- [28] S. Raghu and F. D. M. Haldane, *Phys. Rev. A* **78**, 033834 (2008).
- [29] J. Colpa, *Physica (Amsterdam)* **93A**, 327 (1978).
- [30] M. V. Berry, *Czech. J. Phys.* **54**, 1039 (2004).
- [31] R. J. Hardy, *Phys. Rev.* **132**, 168 (1963).
- [32] T. Qin, Q. Niu, and J. Shi, *Phys. Rev. Lett.* **107**, 236601 (2011).
- [33] R. Shindou, R. Matsumoto, S. Murakami, and J.-i. Ohe, *Phys. Rev. B* **87**, 174427 (2013).
- [34] L. Zhang and Q. Niu, *Phys. Rev. Lett.* **112**, 085503 (2014).
- [35] M. Hirschberger, R. Chisnell, Y. S. Lee, and N. P. Ong, *Phys. Rev. Lett.* **115**, 106603 (2015).
- [36] G. Grosso and G. P. Parravicini, *Solid State Physics*, 2nd ed. (Academic Press, 2013).